

### *Supplementary Information*

#### **Layer-by-layer nanoparticle encapsulating all-trans retinoic acid and CpG as a mucosal adjuvant targeting colorectal cancer**

Shiwei Mi<sup>a,b</sup> Wei Li<sup>a,b</sup> Yixing Wen<sup>a,b</sup> Chen Yang<sup>a,b</sup> Shuai Liu<sup>a</sup> Jingjiao Li<sup>a,b</sup> Xingdi Cheng<sup>a,b</sup>  
Yuanyuan Zhao<sup>a,b</sup> Haonan Huo<sup>a,b</sup> Haowei Zu<sup>a</sup> and Xueguang Lu<sup>a,b,\*</sup>

a. Beijing National Laboratory for Molecular Sciences, CAS Key Laboratory of Colloid, Interface and Chemical Thermodynamics, Institute of Chemistry, Chinese Academy of Sciences, Beijing 100190, China

b. University of Chinese Academy of Sciences, Beijing 100049, China

Email: [xueguang@iccas.ac.cn](mailto:xueguang@iccas.ac.cn)

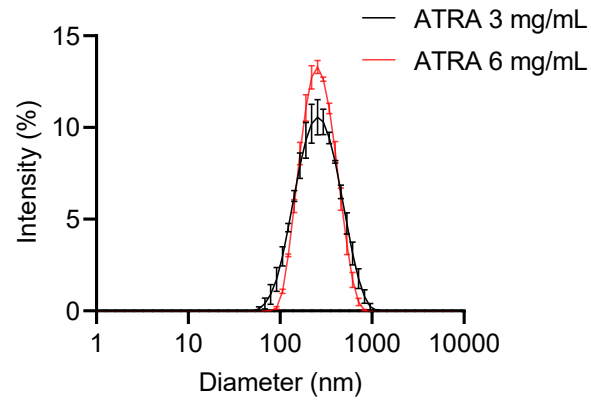
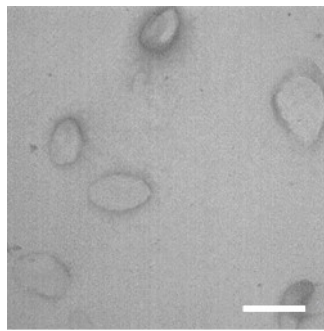


**Figure S1.** Representative size distribution of ATRA-NPs measured by DLS.



ATRA NPs

**Figure S2.** A representative TEM image of ATRA-NPs. The scale bar is 200 nm.

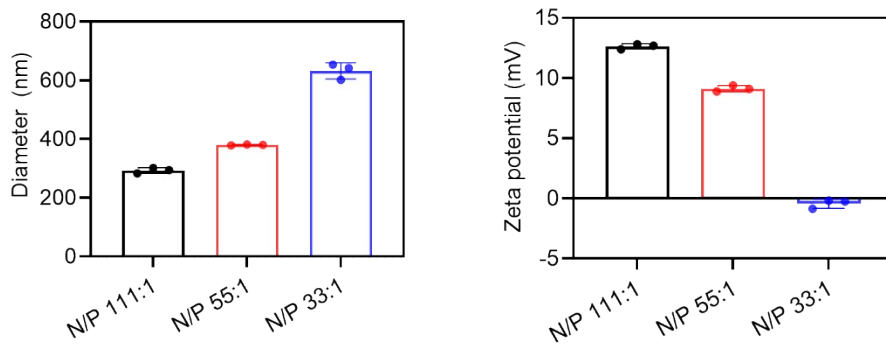


**Figure S3.** The hydrodynamic diameters and zeta potentials of ATRA@CpG-NPs with N/P ratios. n = 3 technical replicates. Data are shown as mean ± SD.

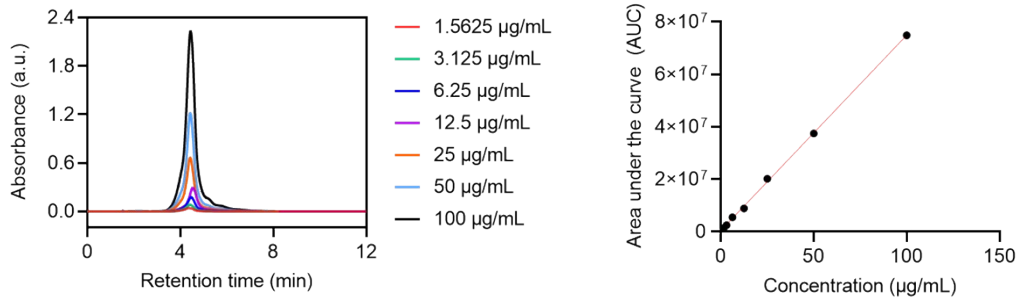


**Figure S4.** Reverse-phase HPLC chromatograms of the ATRA in acetonitrile (left). Standard curve of HPLC AUC over ATRA concentrations.

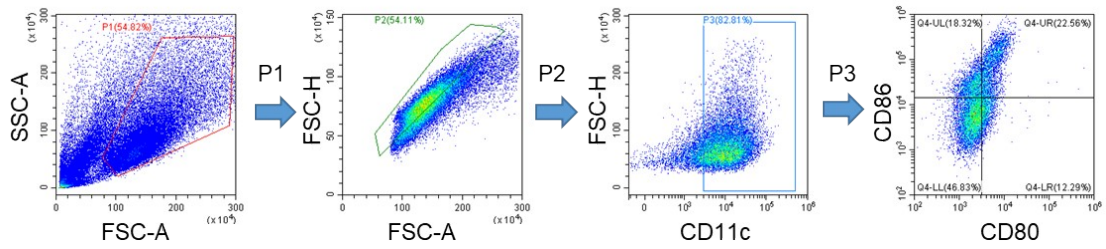


**Figure S5.** Gating strategy for flow cytometry analysis of CD11c<sup>+</sup>CD80<sup>+</sup>CD86<sup>+</sup> cells among BMDCs.

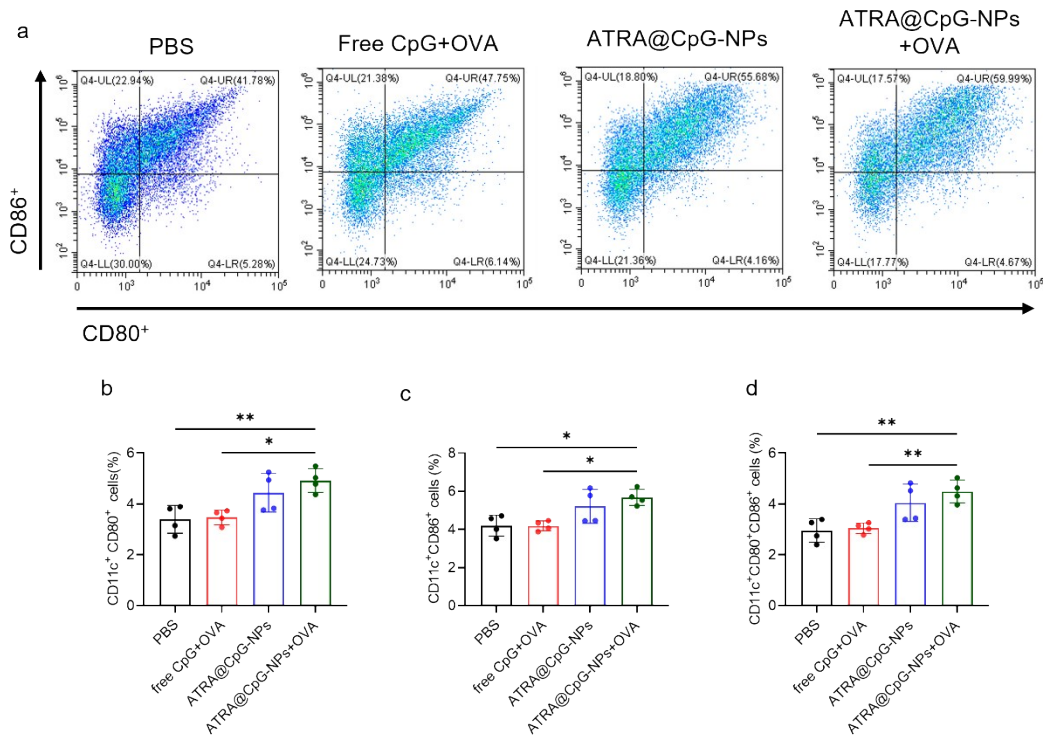


**Figure S6.** (a) Representative flow cytometry plots of CD11c<sup>+</sup>CD80<sup>+</sup>CD86<sup>+</sup> cells. Quantification analysis of CD11c<sup>+</sup>CD80<sup>+</sup> cells (b), CD11c<sup>+</sup>CD86<sup>+</sup> cells(c) and CD11c<sup>+</sup>CD80<sup>+</sup>CD86<sup>+</sup>cells (d). n = 4 technical replicates. Data are shown as mean ± SD. Statistical analysis was performed using one-way analysis of variance (ANOVA) and Tukey's multiple comparisons tests: \*p < 0.05, \*\*p < 0.01.

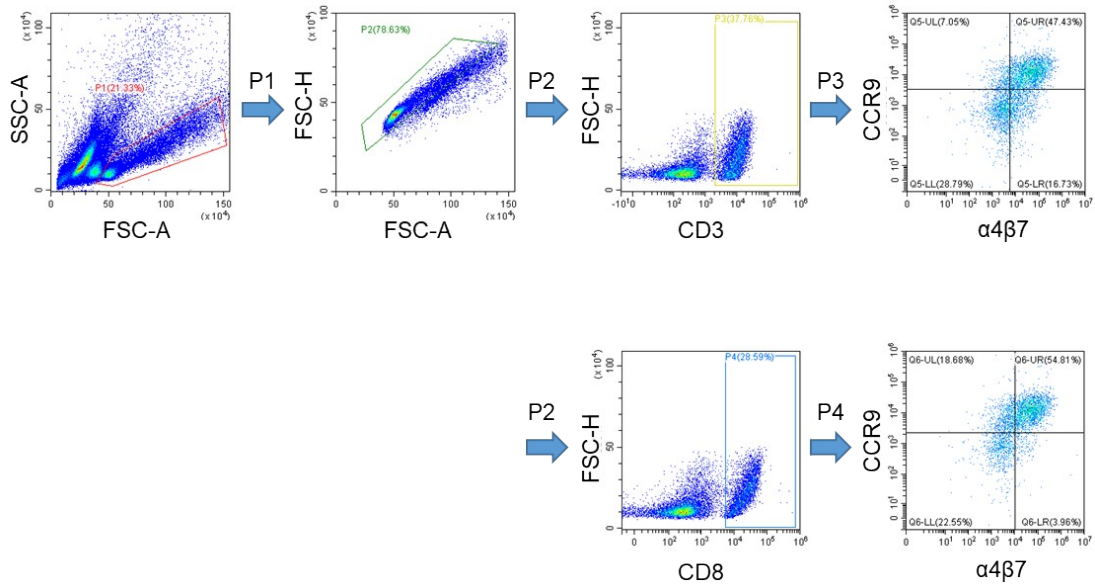


**Figure S7.** Gating strategy for flow cytometry analysis of  $\alpha 4\beta 7^+ \text{CCR}9^+ \text{CD}3^+$  and  $\alpha 4\beta 7^+ \text{CCR}9^+ \text{CD}8^+$  T cells among spleen cells.

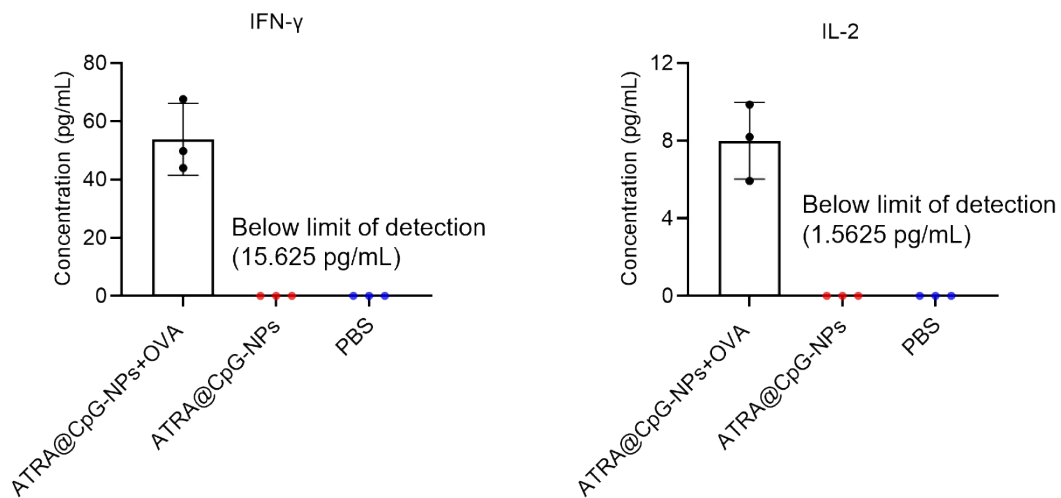


**Figure S8.** IFN- $\gamma$  and IL-2 secretion by OT-1  $\text{CD}8^+$  T cells after 48 h incubation with PBS, ATRA@CpG-NPs and ATRA@CpG-NPs+OVA.  $n = 3$  technical replicates. Data are shown as mean  $\pm$  SD

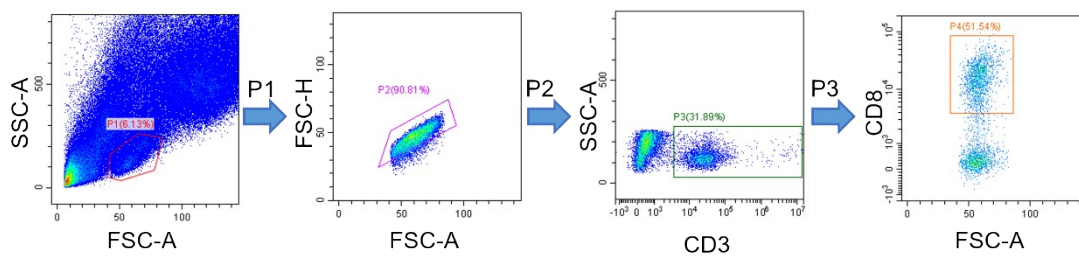


**Figure S9.** Gating strategy for flow cytometry analysis of  $\text{CD}3^+ \text{CD}8^+$  T cells among tumor cells.

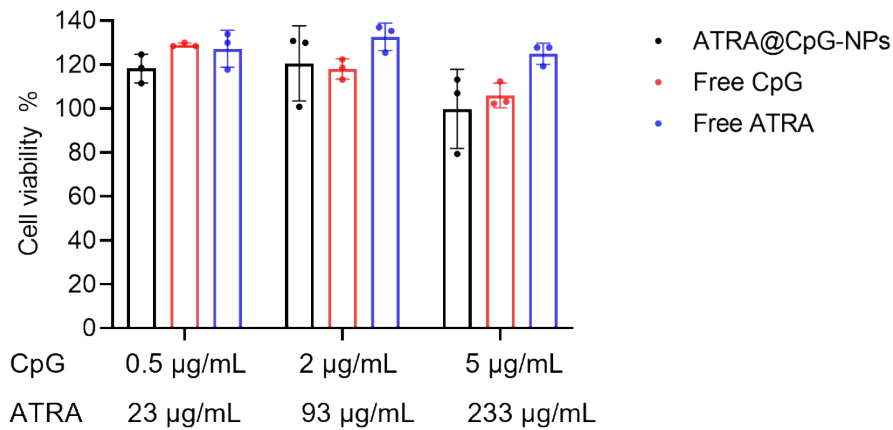


**Figure S10.** The viability of DC2.4 cells after incubation with different concentrations of free CpG, free ATRA and ATRA@CpG-NPs. Data are shown as mean  $\pm$  SD.

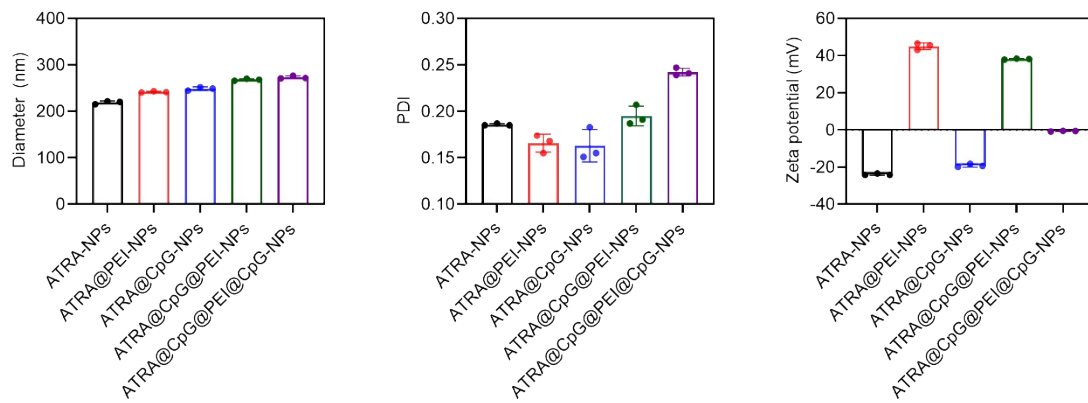


**Figure S11.** The hydrodynamic diameters, polydispersity index and zeta potentials of multiple layered nanoparticles.  $n = 3$  technical replicates. Data are shown as mean  $\pm$  SD.

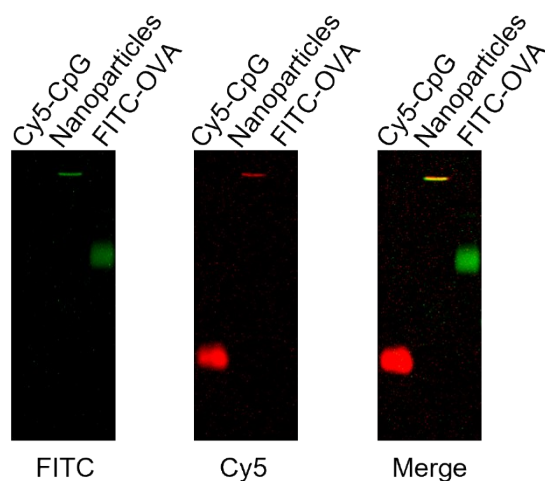


**Figure S12.** Agarose gel (1%) images of Cy5-CpG (red), FITC-OVA (green), and ATRA nanoparticles carrying both CpG and OVA.